Fast prototyping of antenna and FSS structures

TEXTILE ANTENNAS, A PRACTICAL APPROACH

H.J. Visser*, A.C.F. Reniers†

* Holst Centre – TNO
P.O. Box 8550
5605 KN Eindhoven, The Netherlands
E-mail: huib.j.visser@tno.nl

†TNO Science and Industry
P.O. Box 6235
5600 HE Eindhoven, The Netherlands

Keywords: Antenna radiation patterns, Dipole antennas, Human factors, Modelling, Textile antennas.

Abstract

Within the framework of the development of a wearable communications system for a sportsman, a textile antenna has been realised. The required antenna needed to be low profile, washable, insensitive to the proximity of the human skin and relatively insensitive to deformation. To overcome the human operator coupling effects on the antenna input impedance, i.e. a shift in resonance frequency and an increase of return loss level, a practical approach has been chosen. This approach consists of designing an antenna in free space, well matched over a wide frequency band. Because of the requirements and design methodology, chosen was for a (Log Periodic) Folded Dipole Array ((LP)FDA) antenna. Design equations for the antenna are discussed, measurement results of prototype antennas are shown and additional measures to tune the input impedance of the antenna are discussed.

1 Introduction

The progress in electronics miniaturisation has paved the way for the development of portable mobile communications equipment. The next logical step is the development of wearable wireless devices. The need for in-clothing wireless equipment is most obvious in the fields of emergency services and sports where people need the use of both hands and do not want to be hindered by bulky equipment. However, a general consumer-use may be foreseen in the future.

Since in clothing antennas need, preferably, to be easy to integrate into existing clothing and may not impair the mobility of the wearer of the clothing, an 'embroidering' of a wire antenna is preferred. A grounded planar antenna was therefore discarded as a candidate for the sportsman's wearable communications system.

Bringing a (wire) antenna in close proximity to the human operator, however, will significantly affect the antenna characteristics, [1-5]. The effects with respect to the antenna input impedance include a shift in resonance frequency and an increase in the return loss level. A practical approach to deal with these negative effects is to design an antenna in free space that exhibits a good impedance match over a wide frequency bandwidth. The antenna of choice is a linear array of wire folded dipoles.

2 Wire folded dipole array antenna

The folded dipole antenna, see figure 1, is known for its inherent wideband characteristics. This wideband behaviour may be explained by decomposing the current through the antenna into two modes: a dipole antenna mode and a transmission line mode, [6]. The input impedance of an 'ordinary' half-wave dipole antenna is capacitive for frequencies below resonance and inductive for frequencies above resonance. The opposite is true for a short-circuited transmission line stub of a quarter wavelength long. In a folded dipole antenna we may recognise an ordinary half-wave dipole antenna with two series quarter-wave stubs in parallel to the dipole antenna input. The stubs will, to a certain degree, compensate for the change in complex impedance of the dipole antenna around resonance. Thus a wide bandwidth is created in comparison to an 'ordinary' half-wave dipole antenna. An even larger bandwidth may be obtained by creating a series array of folded dipole antennas, where every folded dipole antenna exhibits a different resonance wavelength, see figure 1.

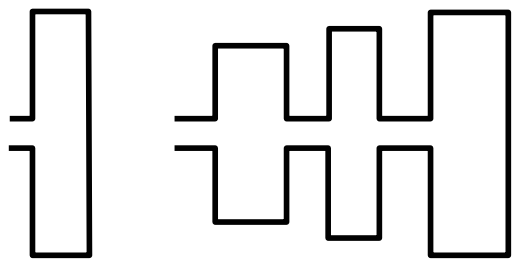

Figure 1: Folded dipole antenna (left) and linear array of folded dipole antennas (right).

2.1 Transmission line model folded dipole antenna

The excitation of a folded dipole antenna may be decomposed into a transmission line mode and an antenna mode, [6], see figure 2. In the most general case, the radii of the wires that make up the folded dipole antenna are not equal, [7]. Here, we will stick to the equal radii folded dipole antenna.

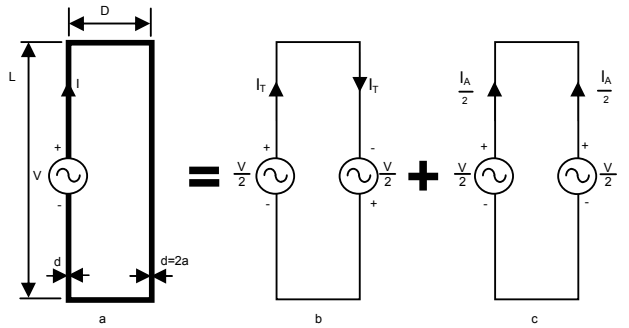

Figure 2: Decomposition of an equal radius wire folded dipole antenna (a) into a transmission line mode (b) and an antenna mode (c).

To obtain the input impedance of a folded dipole antenna as shown in the left of figure 1, where the driven element and the parasitic element have the same wire radius, we start by connecting a voltage source V to the input terminals of the driven element, see figure 2a. The current flowing through the dipole may be decomposed into a transmission line mode and an antenna mode, [6,7].
Figure 2 shows that the total current flowing through the left arm of the folded dipole antenna is $I=I_T+\frac{1}{2}I_A$. The input impedance Z_{in}, therefore is

$$Z_{in} = \frac{V}{I_T + \frac{1}{2} I_A}. \qquad (1)$$

Upon inspection of the transmission line mode, figure 2b, we see a voltage $\frac{1}{2}V$ applied to the upper part of the folded dipole antenna. The current I_T therefore is equal to

$$I_T = \frac{V}{2Z_T}, \qquad (2)$$

where Z_T is the impedance seen looking into the two-wire transmission line stub.
Upon inspection from the antenna mode, figure 2c, we see two equal currents in parallel connected to the same voltage source. Therefore

$$I_A = \frac{V}{2Z_D}, \qquad (3)$$

where Z_D is the impedance of an ordinary cylindrical dipole of equivalent radius a_e and length L. The equivalent radius is calculated from, [6,7]

$$\ln(a_e) = \ln(a) + \frac{1}{2}\ln\left(\frac{D}{a}\right). \qquad (4)$$

Substitution of equations (2) and (3) into equation (1) gives the input impedance of the folded dipole antenna

$$Z_{in} = \frac{4Z_T Z_D}{Z_T + 2Z_D}, \qquad (5)$$

wherein Z_D, the input impedance of a cylindrical dipole antenna of length L and radius a_e, may be calculated by applying the empirical double polyfit equations for the King-Middleton second-order solution as given in [8]. Z_T is the impedance of a short-circuited piece of transmission line of length $\frac{1}{2}L$

$$Z_T = jZ_0 \tan\left(\beta \tfrac{L}{2}\right), \qquad (6)$$

wherein $\beta=2\pi/\lambda$ - assuming a lossless transmission line – and wherein Z_0 is the characteristic impedance of the transmission line. For a two-wire transmission line, [9]

$$Z_0 = 120 \ln\left(\frac{D + \sqrt{D^2 - 2a^2}}{2a}\right). \qquad (7)$$

If we choose the length of the folded dipole antenna to be equal to half a wavelength, Z_T becomes infinite at resonance and the input impedance of the half-wave folded dipole antenna becomes equal to four times the input impedance of the ordinary half-wave dipole antenna.

The linear array of folded dipole antennas as shown in the right of figure 1 does not consist of folded dipoles as just discussed, with exception of the end-element, but does consist of so called re-entrant folded dipole antennas. A re-entrant folded dipole antenna may be analysed though using the results derived for an 'ordinary' folded dipole antenna.

2.2 Re-entrant folded dipole antenna

Figure 3 shows the geometry of a re-entrant folded dipole antenna with the voltage and current definitions.

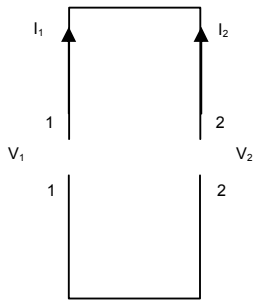

Figure 3: Geometry and voltage and current definitions of a re-entrant folded dipole antenna.

The relations between the currents and voltages are given by

$$\begin{aligned} I_1 &= Y_{11}V_1 + Y_{12}V_2 \\ I_2 &= Y_{21}V_1 + Y_{22}V_2 \end{aligned}. \tag{8}$$

The Y_{11} admittance matrix element is calculated as

$$Y_{11} = \left.\frac{I_1}{V_1}\right|_{V_2=0} = \frac{1}{2}Y_T + \frac{1}{4}Y_D, \tag{9}$$

where use has been made of equation (5) and $Y_T=Z_T^{-1}$ and $Y_D=Z_D^{-1}$. The Y_{22} admittance matrix element follows from short-circuiting port 1-1' and exciting port 2-2': $Y_{22}=Y_{11}$.

The admittance matrix element $Y_{12}=Y_{21}$ is calculated by equalising the two port voltages, $V_1=V_2$. Only the antenna mode will be excited now. Upon substitution of equation (9) into equation (8), we get

$$I_1 = \left(\frac{1}{2}Y_T + \frac{1}{4}Y_D + Y_{12}\right)V_1. \tag{10}$$

From equation (3) we find for the input admittance

$$Y_{in} = Y_D = \frac{2I_1}{V_1}. \tag{11}$$

From equations (10) and (11) the admittance matrix element is calculated as

$$Y_{12} = -\frac{1}{2}Y_T + \frac{1}{4}Y_D. \tag{12}$$

2.3 Linear array of folded dipoles

If we neglect mutual coupling effects between folded dipole elements in a linear array, the input impedance of a series linear array of folded dipoles may be best calculated using ABCD matrices. For the i^{th} folded dipole element in an array consisting of N folded dipole antenna elements, the ABCD matrix is given by

$$\begin{pmatrix} A_i & B_i \\ C_i & D_i \end{pmatrix} = -\frac{1}{Y_{21_i}}\begin{pmatrix} Y_{22_i} & 1 \\ Y_{11_i}Y_{22_i} - Y_{21_i}Y_{12_i} & Y_{11_i} \end{pmatrix}, \tag{13}$$

where Y_{abi}, $a,b=1,2$, $i=1,2,\ldots,N$ are given by equations (9) and (12).

The ABCD matrix of a length of transmission line in between two folded dipole antennas is given by, [10]

$$\begin{pmatrix} A_m & B_m \\ C_m & D_m \end{pmatrix} = \begin{pmatrix} \cosh(\gamma_m l_m) & Z_{0m}\sinh(\gamma_m l_m) \\ \dfrac{\sinh(\gamma_m l_m)}{Z_{0m}} & \cosh(\gamma_m l_m) \end{pmatrix}, \tag{14}$$

for $m=1,2,\ldots,N-1$. Herein is l_m the length of the piece of transmission line m, Z_{0m} is the characteristic impedance and γ_m is the propagation constant.

The ABCD matrix of a series load, Y_L, (e.g. a short-circuit) at the end of the array is given by

$$\begin{pmatrix} A_L & B_L \\ C_L & D_L \end{pmatrix} = \begin{pmatrix} 1 & 0 \\ Y_L & 1 \end{pmatrix}. \tag{15}$$

The complete array is characterised by

$$\begin{pmatrix} A & B \\ C & D \end{pmatrix} = \prod_{n=1}^{2N}\begin{pmatrix} A_n & B_n \\ C_n & D_n \end{pmatrix}. \tag{16}$$

The impedance matrix is then given by

$$\begin{pmatrix} Z_{11} & Z_{12} \\ Z_{21} & Z_{22} \end{pmatrix} = \frac{1}{C}\begin{pmatrix} A & AD-BC \\ 1 & D \end{pmatrix}. \tag{17}$$

3 Model verification

The theory describing the folded dipole antenna and series array of re-entrant folded dipoles has been implemented in software. For the equivalent dipole analysis, the empirical double polyfit equations for the King-Middleton second-order solution as given in [8] have been used. Furthermore, an extended length has been introduced to account for the folded dipole end effect, allowing a wire separation up to a sixth of a wavelength, [11].

Figure 4 shows the real and imaginary part of the input impedance of a single folded dipole antenna as function of frequency. These results, obtained with the transmission line (TL) model, are compared with results from a Method of Moments (MoM) analysis, shown in the same figure. The dimensions of the antenna, see figure 2, are stated in the figure caption.

All calculations have been performed for Perfect Electric Conductors (PECs), but a MoM analysis of the same structure consisting of copper wires gave results very similar to the ones shown in figure 4.

The figure clearly demonstrates the validity of the TL model for frequencies around resonance. The benefit of the TL calculations over MoM simulations lies in the computation time.

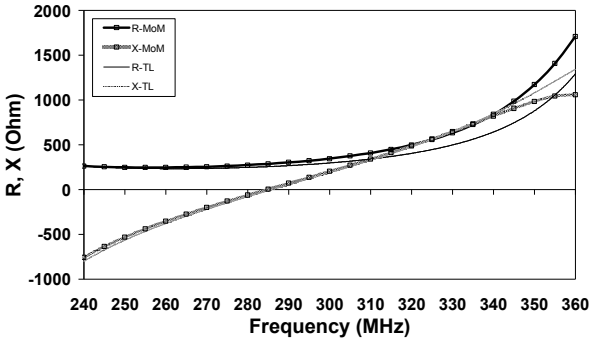

Figure 4: Real and imaginary parts of the input impedance of a folded dipole antenna vs. frequency. Antenna dimensions: *L=0.5m*, *a=0.0001m*, *D=0.005m*.

Figures 6 to 8 show the TL input impedance vs. frequency results for a two element folded dipole array antenna, shown in figure 5. The antennas for which the analysis results are shown in figures 6 to 8 only differ in the distance L between the two folded dipole antenna elements. The dimensions of the array antennas are given in the figure captions. The lengths of both folded dipole antenna elements are, respectively, L_1 and L_2. For both folded dipoles, the wire radius is a and the wire separation is D. The length of the transmission line between the two folded dipoles is L.

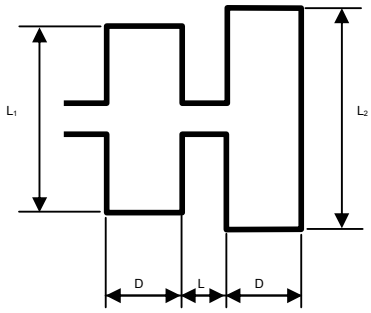

Figure 5: Two-elements folded dipole array antenna.

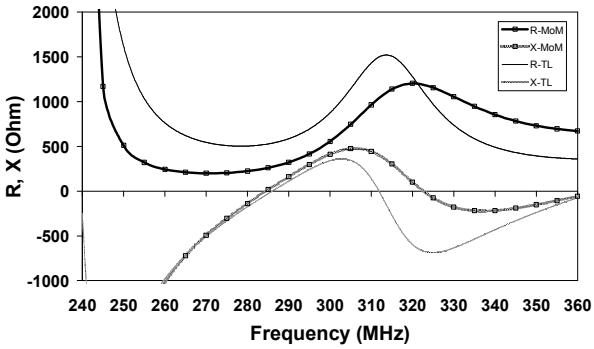

Figure 6: Real and imaginary parts of the input impedance of a two-elements folded dipole array antenna vs. frequency. Antenna dimensions: *L_1=0.4m, L_2=0.5m*, *a=0.0001m*, *D=0.005m, L=0.2m*.

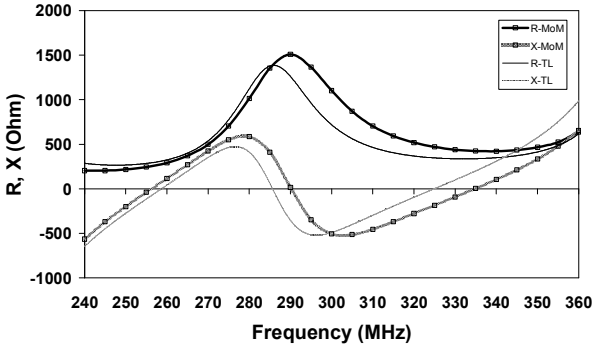

Figure 7: Real and imaginary parts of the input impedance of a two-elements folded dipole array antenna vs. frequency. Antenna dimensions: *L_1=0.4m, L_2=0.5m*, *a=0.0001m*, *D=0.005m, L=0.4m*.

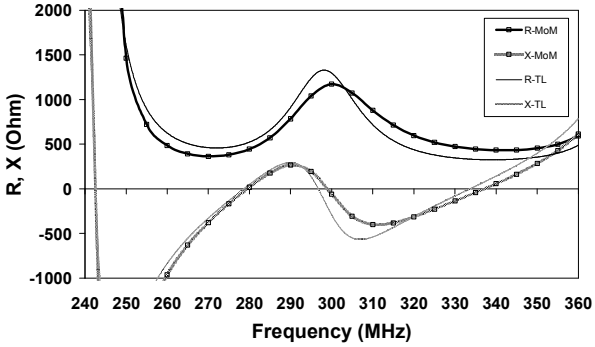

Figure 8: Real and imaginary parts of the input impedance of a two-elements folded dipole array antenna vs. frequency. Antenna dimensions: *L_1=0.4m, L_2=0.5m*, *a=0.0001m*, *D=0.005m, L=0.84m*.

The figures show that the analysis results get better with increasing separation of the folded dipole antenna elements in the array. This is consistent with the fact that mutual coupling effects are not accounted for in the TL analysis. Furthermore, analysis results are shown for rather thin wires. For thick wires, the agreement with MoM results is not as good as shown in these figures. A replacement of the dipole analysis with one better fit for handling thicker wires, e.g. a MoM analysis, is believed to cure this problem. Nevertheless, the method is believed to be accurate enough for creating initial wire folded dipole array antenna designs very fast.

4 Prototype antennas

With the transmission line model it should be possible to design a broadband wire antenna. In a log-periodic array configuration the array antenna performance is periodic as a function of the logarithm of the frequency. Thus a wide frequency band may be created. The lengths of the folded dipole elements in a linear array as shown in figure 1 therefore need to increase logarithmically and the same applies for the inter-element distances. The meander-line

reversal that may be observed in the linear array, automatically provides for a 180^0 phase reversal between the array elements, [7]. This phase reversal makes that the interference between adjacent array elements is minimal and that the beam of the array antenna is an endfire beam in the direction of the shorter elements. These features make the Log-Periodic Folded Dipole Array (LPFDA) antenna a good choice for an upper-arm or shoulder based in-clothing antenna. The TL model should be able to predict the LPFDA antenna behaviour.

In parallel to the development of the analysis software described, experimental work has been carried out on LPFDA antennas. These antennas were designed for free space, using the antenna dimensional constraints outlined in [7]. Next, these antennas were brought close to the human skin, to examine the effects of a human operator on input impedance as function of frequency and on radiation characteristics.

4.1 868MHz copper tape antenna

Figure 9 shows a photograph of a two-element LPFDA antenna, made out of copper tape, attached to the shoulder of a cotton shirt. The antenna is designed to operate in a frequency band around *868MHz*. The shirt is draped over a balloon filled with salt water in an attempt to mimic the human torso. For that same reason, during measurements, another balloon filled with salt water was positioned on top in an attempt to mimic the human head.

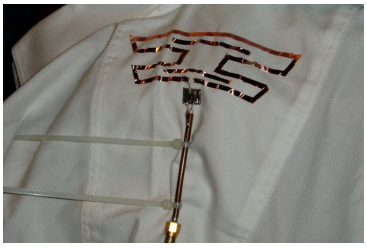

Figure 9: Two-element LPFDA antenna made out of copper tape, attached to a cotton shirt.

The radiation patterns, normalised to their own maximum values, in the *E*-plane, are shown in figure 10 for some frequencies.

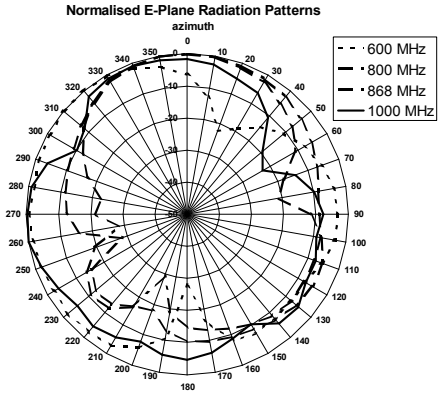

Figure 10: Normalised *E*-plane radiation patterns for two-element *868MHz* LPFDA antenna.

The *H*-plane radiation patterns are shown in figure 11.

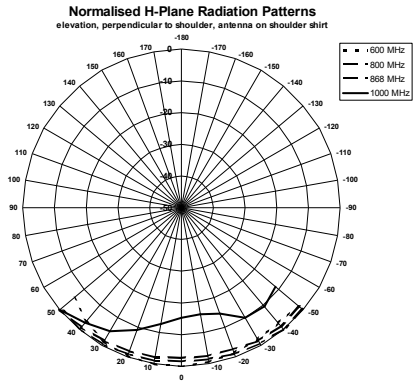

Figure 11: Normalised *H*-plane radiation patterns for two-element *868MHz* LPFDA antenna.

The figures show that in a large frequency band around *868MHz* the radiation pattern is undisturbed in a cone with an opening angle of about 80^0. Note that the 0^0 position in figure 11 is not identical to the 0^0 position in figure 10.

4.1 2.4GHz embroidered antenna

Next, an LPFDA antenna was designed for a frequency band around *2.45GHz* and embroidered into a piece of cotton cloth, see figure 12.

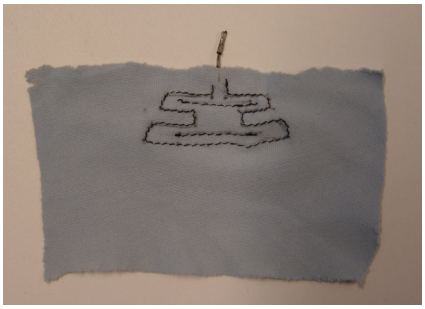

Figure 12: Two-element LPFDA antenna made out of an electrically conducting thread, embroidered in a piece of cotton cloth.

The thread used for embroidering the antenna consists of a combination of stainless steel fibres.

In figure 13, the measured return loss as function of frequency is shown for the antenna in free space and for the antenna attached to a human arm.

As figure 12 shows, the tolerances on the antenna dimensions in the construction of the two-element LPFDA antenna have not been very tight. The stretching of the cotton cloth during fabrication is the reason for this. The main effect is shown in figure 13 as a change in resonance frequency from the required *2.45GHz* for the antenna in free space. Further, the measurements turned out to be very sensitive to the wire spacing in the piece of two-wire transmission line shown at

the top of figure 12. This spacing was kept constant by applying a piece of tape to the transmission line.

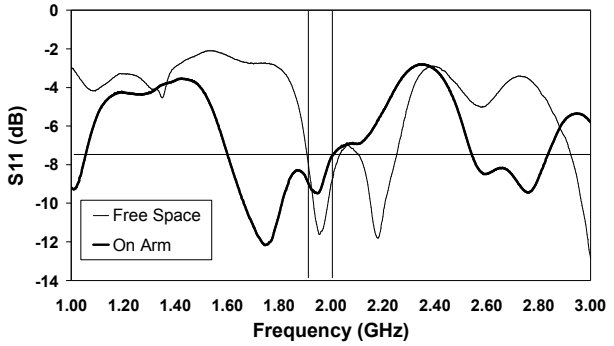

Figure 13: Measured return loss vs. frequency in free space and on-arm for a two-element LPFDA antenna embroidered in a piece of cotton cloth.

Notwithstanding all these negative effects, figure 13 shows that the proposed design strategy, i.e. designing an over-wide-band antenna in free space to overcome the frequency shift due to the presence of the human operator, does work.
If we settle for a return loss better than -*7.5dB*, we see that – in a small frequency range – the antenna is still matched when brought close to the human operator.
The figure also shows that additional measures must be taken to improve the impedance match over a wider frequency band.

5 Impedance matching measures

From a practical point of view, a uniform wire radius in every folded dipole antenna element and in every piece of two-wire transmission line should be used. This allows for embroidering antennas in clothing, using a single thread. As a drawback however, we do not have the step-up impedance ratio, [6,7], at our disposal to help in tuning the input impedance. This leaves us, in a folded dipole array antenna, basically with the wire separations in the folded dipoles and the interconnecting transmission lines and the folded dipole separations as parameters to tune the input impedance. The folded dipole lengths are mainly for determining the resonance frequencies within the frequency band of interest.

For folded dipole array antennas with only a few elements or for single folded dipole antennas we would like to have more input impedance tuning options at our disposal. We have found these options in either positioning short circuits in the arms of the folded dipole or in loading the folded dipole with parasitic dipoles or parasitic folded dipoles. Of course, both methods can be applied at the same time.

4.1 Short circuits

As we have seen, the folded dipole antenna may be analysed by decomposing the current flowing through the antenna in a transmission line mode and an antenna mode. This decomposition opens up the possibility to either act in the transmission line mode or in the antenna mode to tune the input impedance. We may act in the transmission line mode by placing short circuits in the arms of the folded dipole antenna, see figure 14. In doing so, we shorten the stub lengths but keep the dipole antenna mode intact. In the analysis, we only need to replace the length L in equation (6) with L', see figure 14.

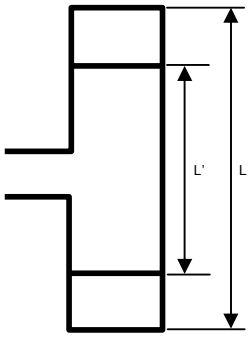

Figure 14: Folded dipole antenna with additional short-circuits.

To validate the above, a number of configurations have been analysed and compared with MoM analysis results. Figures 15 and 16 show two examples based on the configuration without short-circuits for which the analysis results are shown in figure 4.

These figures, together with figure 4, show first of all that our assumption that only the transmission line mode is affected is correct and further they show that the input impedance can be adjusted over a large dynamic range. Note, that no attempt has been made to tune the input impedance to a certain value. The graphs are presented just to show the possibility of tuning with positioning short-circuits in the arms of a folded dipole antenna.

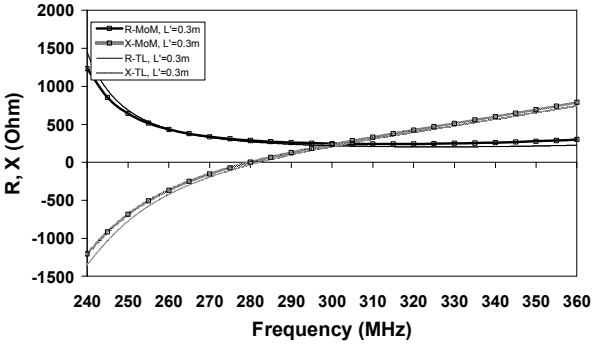

Figure 15: Real and imaginary parts of the input impedance of a folded antenna with short circuits vs. frequency. Antenna dimensions: *L=0.5m*, *a=0.0001m*, *D=0.005m*, *L'=0.3m*.

Another tuning mechanism may be provided by acting in the antenna mode through placing parasitic elements in close proximity to a folded dipole antenna.

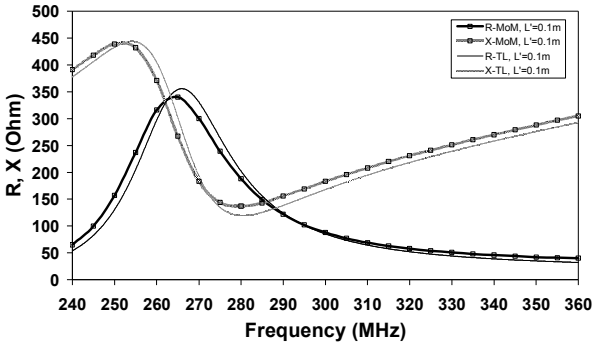

Figure 16: Real and imaginary parts of the input impedance of a folded antenna with short circuits vs. frequency. Antenna dimensions: *L=0.5m*, *a=0.0001m*, *D=0.005m*, *L'=0.1m*.

4.2 Parasitic elements

We may tune the input impedance of a folded dipole antenna by placing a short circuited dipole or folded dipole in close proximity to the folded dipole antenna, see figure 17.

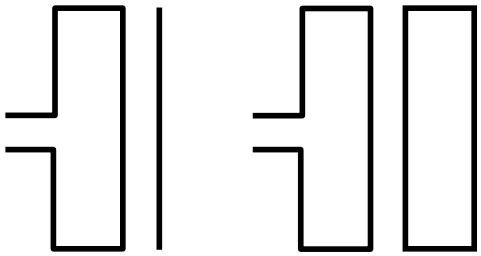

Figure 17: Short-circuited dipole (left) or short-circuited folded dipole (right) coupled to a folded dipole antenna.

The input impedance of the folded dipole antenna is

$$Z_{in} = Z_{11} - \frac{Z_{12}Z_{21}}{Z_{22}}, \qquad (18)$$

wherein Z_{11} is the input impedance of the isolated folded dipole antenna, Z_{22} is the input impedance of the isolated dipole antenna and, [12], for the dipole antenna coupled to the folded dipole antenna

$$Z_{12} = Z_{21} = 2 \cdot Z_{21_{dipole-to-dipole}}. \qquad (19)$$

Herein, $Z_{21dipole\text{-}to\text{-}dipole}$ is the mutual impedance between two 'ordinary' dipole antennas. This impedance may be calculated (for thin wires) using the closed form equations of [13].

For the short-circuited folded dipole coupled to the folded dipole antenna, equation (18) holds, but now Z_{22} is the input impedance of the isolated folded dipole antenna and, [12]

$$Z_{12} = Z_{21} = 4 \cdot Z_{21_{dipole-to-dipole}} \qquad (19)$$

Herein, $Z_{21dipole\text{-}to\text{-}dipole}$ is, again, the mutual impedance between two 'ordinary' dipole antennas.

To validate the above, a number of configurations have been analysed and compared with MoM analysis results. Figures 18 and 19 show two examples for a short-circuited dipole coupled to the folded dipole antenna. The configurations analysed are based on the configuration without parasitic elements for which the analysis results are shown in figure 4.

The length of the folded dipole antenna is L_{fd}, the length of the short-circuited parasitic dipole is L_d, the center-to-center separation between folded dipole antenna and parasitic element is L. all wires have equal radius a.

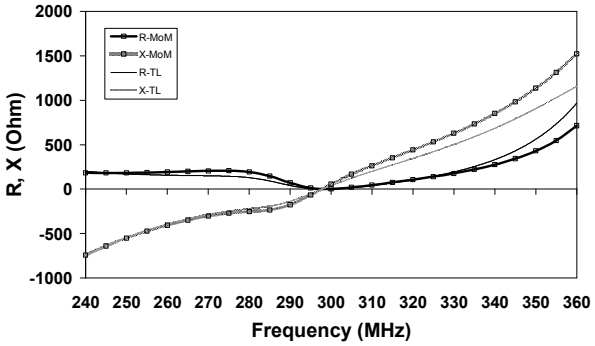

Figure 18: Real and imaginary parts of the input impedance vs. frequency of a folded antenna with a parasitic short – circuited dipole. Antenna dimensions: L_{fd}=*0.5m*, L_d=*0.5m*, *a=0.0001m*, *D=0.005m*, *L=0.01m*.

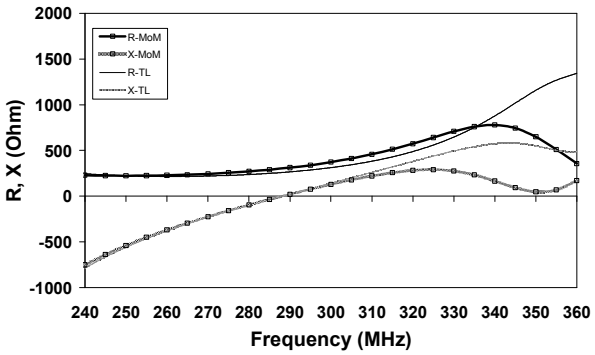

Figure 19: Real and imaginary parts of the input impedance vs. frequency of a folded antenna with a parasitic short – circuited dipole. Antenna dimensions: L_{fd}=*0.5m*, L_d=*0.4m*, *a=0.0001m*, *D=0.005m*, *L=0.02m*.

The figures show that the input impedance may be adjusted by using parasitic elements, using the length and distance to the folded dipole for the required result. Note, that again no

attempt has been made to tune the input impedance to a certain value.

6 Conclusions

To overcome human operator coupling effects on textile antennas, a practical design approach may be used. Antennas are designed in free space, well matched over a wide frequency band. Thus the coupling effects, a shift in resonance frequency and an increase of return loss levels may be compensated for. Because of the ease in fabrication and the chosen design methodology, (Log Periodic) Folded Dipole Array antennas are considered an optimum choice. Design equations for this antenna type have been derived and verified as well as new means of impedance tuning.

References

[1] H. –R. Chuang, "Human Operator Coupling Effects on Radiation Characteristics of a Portable Communication Dipole Antenna", *IEEE Trans. Ant. Propag.*, Vol. 42, No. 4, pp. 556-560, (1994).

[2] P. Salonen and J. Rantanen, "A Dual-Band and Wide-Band Antenna on Flexible Substrate for Smart Clothing", *IEEE Ind. Electr. Soc. Conf.*, pp. 125-130, (2001).

[3] T. Onishi and K. Ito, "Consideration of Antennas Close to Lossy Objects", *Ant. Propag. Int. Symposium*, pp. 440-442, (2002).

[4] W. G. Scanton and N. E. Evans, "Numerical Analysis of Bodyworn UHF Antenna Systems", *Electronics and Communication Engineering Journal*, pp. 53-64, (2002).

[5] J. R. Verbiest and G. A. E. Vandenbosch, "A Novel Small-Size Printed Tapered Monopole Antenna for UWB WBAN", *IEEE Ant. Wireless Propag. Letters*, Vol. 5, pp. 377-379, (2006).

[6] W. L. Stutzman and G. A. Thiele, "*Antenna Theory and Design, 2nd edition*", John Wiley & Sons, New York, (1997).

[7] R. C. Johnson, "*Antenna Engineering Handbook, 3rd edition*", McGraw-Hill, New York, (1993).

[8] R. S. Elliot, "*Antenna Theory and Design, revised Edition*", John Wiley & Sons, New York, (2003).

[9] G. A. Thiele, E. P. Ekelman, Jr. and L. W. Henderson, "On the Accuracy of the Transmission Line Model of the Folded Dipole", *IEEE Trans. Ant. Propag.*, Vol. AP-28, No. 5, pp. 700-703, (1980).

[10] K. C. Gupta, R. Garg and R. Chadha, "Computer Aided Design of Microwave Circuits", Artech House, Dedham, (1981).

[11] A. R. Clark and A. P. C. Fourie, "An Improvement to the Transmission Line Model of the Folded Dipole", *IEE Proceedings –H*, Vol. 138, No. 6, pp. 577-579, (1991).

[12] A. R. Clark and A. P. C. Fourie, "Mutual Impedance and the Folded Dipole", *2nd Int. Conf. Computation in Electromagnetics*, pp. 347-350, (1994).

[13] H. E. King, "Mutual Impedance of Unequal Length Antennas in Echelon", *IRE Trans. Ant. Propag.*, pp. 306-313, (1957).

.